Inter-Vehicular Communication using IEEE 802.16e Technology

Raúl Aquino-Santos[1], Luis A. Villaseñor-González[2], Víctor Rangel-Licea[3], Arthur Edwards-Block[1], Alejandro Galaviz-Mosqueda[2], Luis Manuel Ortiz Buenrostro[3]

[1]*University of Colima, Av. Universidad 333, C.P. 28045, Colima, Colima, México*
[2]*CICESE, Research Centre, Carr. Tijuana-Ensenada #3918, Ensenada, B. C., México*
[3]*National Autonomous University of Mexico (UNAM), Mexico, D.F.*

Abstract: This chapter evaluates a novel uncoordinated WiMAX-mesh model that has been proposed for inter-vehicular communication. To validate our WiMAX-mesh model, extensive simulations have been realized in OPNET modeler. In addition, to demonstrate the applicability of the mobile routing algorithms in vehicular ad hoc networks, the Ad hoc On-Demand Distance Vector (AODV) and the Optimized Link State Routing (OLSR) protocols are compared in detail in a simulated motorway environment with its associated high mobility. A microscopic traffic model developed, also in OPNET, has been used to ascertain the mobility of 100 vehicles on a four-lane motorway. Finally, the mobile ad hoc routing algorithms were evaluated over our proposed WiMAX-mesh model in terms of delivery ratio, delay, routing overhead, routing load, overhead, WiMAX delay, load and throughput.

Keywords: Inter-Vehicular Communication, Vehicular Ad Hoc Networks, IEEE 802.16e, VANETs, Microscopic Traffic Models.

1. INTRODUCTION

In order to reduce the number of vehicular accidents, computer and network experts propose active safety systems, including Intelligent Transportation Systems (ITS) that are based on Inter-Vehicle Communication (IVC) and Vehicle-to-roadside Communication (VRC). Presently, technologies related to these architectures and their related technologies may, in the future, have significant applications in the area of efficiently administering traffic flow, which, in turn, can have important economic and safety ramifications.

Active vehicular systems employ wireless ad hoc networks and Geographic Positioning Systems (GPS) to determine and maintain the inter-vehicular distancing necessary to insure both the one hop and multi hop communications needed to maintain spacing between vehicles. Location-based routing algorithms form the basis of any Vehicular Ad hoc Network (VANET) because of the flexibility and efficiency they provide in inter-vehicular communication systems. Several location-based routing algorithms presently exist, including Grid Location Service (GLS), Location Aided Routing (LAR), Greedy Perimeter Stateless Routing (GPSR), Distance Routing Effect Algorithm for Mobility (DREAM) and Location-Based Routing Algorithm with Cluster-Based Flooding (LORA-CBF). However, to the best of our knowledge, research has been conducted mainly using well-known IEEE 802.11 technology. This chapter proposes employing WiMAX (Worldwide Interoperability for Microwave Access), an increasing important wireless communication system that is expected to provide high data rate communications in metropolitan area networks (MANs). In the past few years, the IEEE 802.16 working group has developed a number of standards for WiMAX. The first standard was published in 2001, which supports communications in the 10-66 GHz frequency band. In 2003, IEEE 802.16a was introduced to provide additional physical layer specifications for the 2-11 GHz frequency band. These two standards were further revised by IEEE 802.16-2004. Recently,

IEEE 802.16e was approved as the official standard for mobile applications.

Generic routing protocols have the design goals of optimality, simplicity and low overhead, robustness and stability, rapid convergence, and flexibility. However, since mobile nodes have less available power, processing speed, and memory, low overhead becomes more important than in fixed networks. The high mobility present in vehicle-to-vehicle communication also places great importance on rapid convergence. Therefore, it is imperative that ad hoc protocols deal with any inherent delays in the underlying technology, deal with varying degrees of mobility, and be sufficiently robust in the face of potential transmission loss due to drop out. In addition, such protocols should also require minimal bandwidth and efficiently route packets.

Several routing algorithms for ad hoc networks have emerged recently to address difficulties related to unicast routing. Such algorithms can be categorized as either proactive or reactive, depending on their route discovery mechanism.

This chapter presents a set of performance predications for ad hoc routing protocols used in highly mobile vehicle-to-vehicle multi-hop networks as part of the extensive research and development effort which will be undertaken in the next decade to incorporate wireless ad hoc networking in the automobile industry.

In order to evaluate this work, Ad hoc On-demand Distance Vector (AODV) routing algorithm, and the Optimized Link State Routing (OLSR) protocol, are compared. Our WiMAX-mesh model applies to vehicles on a motorway, uses a constant traffic model and uses a proto-c code in OPNET. Our simulation evaluates delivery ratio, delay, routing overhead, routing load, overhead, WiMAX delay, load and throughput.

The remainder of this chapter is organized as follows. Section 2 presents a brief introduction to inter-vehicle and vehicle-to-roadside communication. Section 3 describes the IEEE 802.16e standard. Section 4 reviews mobile ad hoc routing algorithms. Section 5 presents the microscopic traffic simulation model. Section 6 describes the simulated scenario. Section 7 reviews the simulation metrics and Section 8 presents results, conclusions and future work.

2. INTER-VEHICLE AND VEHICLE-TO-ROADSIDE COMMUNICATIONS

The last decade has witnessed an increased interest in inter-vehicle and vehicle-to-roadside communication, in part, because of the proliferation of wireless networks. Most research in this area has focused on vehicle-roadside communication, also called beacon-vehicle communication [1, 2] in which vehicles share the medium by accessing different time slots (Time Division Multiple Access, TDMA), beacons (down-link direction) and vehicles (up-link direction).

Some common applications for vehicle-to-roadside communications with limited communication zones of less than 60 meters include: Automatic Payment, Route Guidance, Cooperative Driving, and Parking Management, among others. However, with the introduction of the IEEE 802.11 standard, wireless ad hoc networks and location-based routing algorithms have made vehicle-to-vehicle communication possible [3, 4].

The authors in [3] compare a topology-based approach and a location-based routing scheme. The authors chose Greedy Perimeter Stateless Routing (GPSR) as the location-based routing scheme and Dynamic Source Routing (DSR) as the topology-based approach. In [4], the authors compare two topology-based routing approaches, DSR and Ad hoc On-Demand Distance Vector (AODV), versus one position-based routing scheme, GPSR, in an urban environment.

In inter-vehicle communication, vehicles are equipped with on-board computers and

wireless networks, allowing them to contact other similarly equipped vehicles in their vicinity. By exchanging information, in the near future, vehicles will be able to obtain knowledge about local traffic conditions, which may improve comfort, traffic flow and safety.

The focus of this chapter is inter-vehicle communication because vehicle-roadside communication has already been proposed for standardization in Europe (CEN TC 278 WG 9) and North America (IVHS).

3. IEEE 802.16e STANDARD

A great demand for fast Internet access, voice and video applications, combined with the global tendency to use wireless devices, has increased the significance of Broadband Wireless Access (BWA) networks. Unlike other broadband technologies, such as xDSL (Digital Subscriber Line), FITL (Fiber In The Loop), WITL (Wireless In The Loop) among others, BWA networks are easier to implement and expand, they do not require a large initial investment and have low maintenance costs. In addition, BWA networks are easy to update and promise to have a promising future due to the growing demand for broadband access.

Nevertheless, it was not until only a decade ago that some international institutions began to standardize this type of technology. The first attempt of a BWA system was the Wireless ATM protocol [5], but the lack of industry support led this system to be an unviable broadband solution for residential users.

However, a promising solution for broadband wireless access is the IEEE 802.16 protocol that was developed at the beginning of this decade by hundreds of engineers from the world's leading operators and vendors, as well as by many academic researchers.
The first version of this protocol, IEEE 802.16-2001 [6], was standardized in April, 2002, and supports data rates of up to 134 Mbps in a 28MHz channel with a 30-mile range. At the beginning of its development, this protocol was oriented for fixed wireless users with line of sight (LOS), using the 11-66 GHz spectrum range. Of significance, in 2004, the aim of this protocol was changed to support residential access and NLOS.

WIMAX´s second version, IEEE 802.16-20004 [7], supports two Media Access Control topologies: 1) point to multipoint (PMP), where traffic only occurs between a Base Station (BS) and Subscriber Stations (SS), and 2) Mesh topology, where traffic can be routed through other SSs and can occur directly between SSs. The mesh mode is the extension of the PMP mode, with the advantage of less coverage path loss. Also, the coverage and robustness improve as subscribers are added. In the mesh mode, system throughput can be increased by using multiple-hop paths [8] [9]. Thus, Wireless Mesh Networks (WMNs) can be used to extend cell ranges, cover shadowed areas and enhance system throughput. In addition, the second version also includes OFDM modulation and supports 256 carriers, which considerably reduces multipath fading effects.

Recently, the IEEE 802.16 Task Force released a new version of this standard that enables mobility in SSs. This new IEEE 802-16e [10] standard promises mobility support for speeds up to 120 km/h, along with an asymmetrical link structure. It will enable a SS to be operated as a PDA, phone or laptop. The following section presents a description of the IEEE 802.16 protocol.

3.1 IEEE 802.16e Standard description

The IEEE 802.16e standard uses the same Medium Access Control (MAC) protocol defined in IEEE 802.16 [7], with several different physical layer specifications that depend on the spectrum used and the associated regulations. In general, the MAC protocol defines both frequency division duplex (FDD) and time division duplex (TDD). Transmissions from a Base Station (BS) to Subscriber Stations (SSs) are conducted by a Downlink (DL) Channel,

using PMP wireless access that employs a frequency channel for FDD or a time signaling frame for TDD.

In the mobile version (IEEE 802.16e), Multiple SSs share one slotted uplink (UL) channel via TDD on a demand basis for voice, data, and multimedia traffic. Upon receiving the demand for bandwidth, the BS handles bandwidth allocation by assigning uplink grants based on requests from SSs. A typical signaling frame for TDD includes a DL sub-frame and a UL sub-frame. In turn, the DL sub-frame includes a preamble, Frame Control Header (FCH), and a number of data bursts for SSs, as depicted in Figure 1. The Preamble is used for synchronization and equalizations, and contains a predefined sequence of well-known symbols at the receiver. The FCH specifies the burst profile and length of at least one downlink burst immediately following the FCH. The DL-MAP and UL-MAP frames are MAC management messages that include information elements (IE) that define the access and the burst start time in the downlink and uplink direction, respectively. These frames are broadcast by the BS following the transmission of the FCH sub-frame.

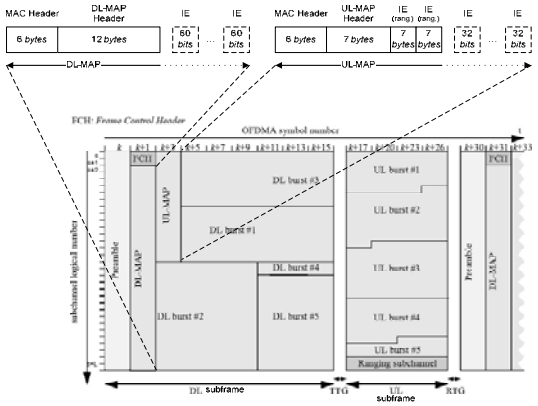

Figure 1: Frame structure for IEEE 802.16e MAC protocol.

Upon entering the BWA network, each SS must go through the Initialization and Registration setup illustrated in Figure 2. The DCD and the UCD are the downlink and uplink channel descriptors, respectively, that provide channel profile information, such as frequency, Channel ID, mini-slot size, symbol rate, etc. On power-up, subscriber stations need to synchronize with a DL channel and an UL channel.

When a SS has tuned to a DL channel, it gets the frame structure of the UL channel, called a UL-MAP frame. Then the ranging procedure is performed, where the round-trip delay and power calibration are determined for each SS, so that SS transmissions are aligned with the BS receive frame for OFDMA PHY and received within the appropriate reception thresholds. This procedure is carried out using the ranging request (RNG-REQ) and the ranging response (RNG-RPS) messages.

The following step is to negotiate basic capabilities such as duplex mode (full or half), modulation and demodulation types (BPSK, QPSK, 16-QAM, and 64-QAM), UL and DL FEC types, and maximum transmission power, among others. This procedure is carried out by exchanging the SBC-REQ and the SBC-RSP messages.

After this, the next step is to carry out the authorization and the key exchange procedure, so that the BS authenticates the SS´s identity and provides the SS with an authorization key (AK). Following this, the registration procedure is performed, where a SS receives a Secondary Management CID (Connection Identifier) that allows it to enter the network and become manageable. This procedure is performed by exchanging the REG-REQ and REG-RSP messages.

Next, IP connectivity must then be established. The Base Station (BS) then uses the DHCP mechanisms in order to obtain an IP address for the SS and meet any other parameters needed to establish IP connectivity. Then, the SS establishes the time of the day, which is required for time-stamping logged events and key management.

Following this, the SS establishes a security association and transfers control parameters via TFTP. These parameters determine the BS and SS capabilities, such as QoS

parameters, fragmentation and packing, among others. Finally, the BS establishes connections for pre-provisioned service flows belonging to the SS by exchanging Dynamic Service Addition Request (DSA-REQ) and DSA Response (DSA-RSP) messages.

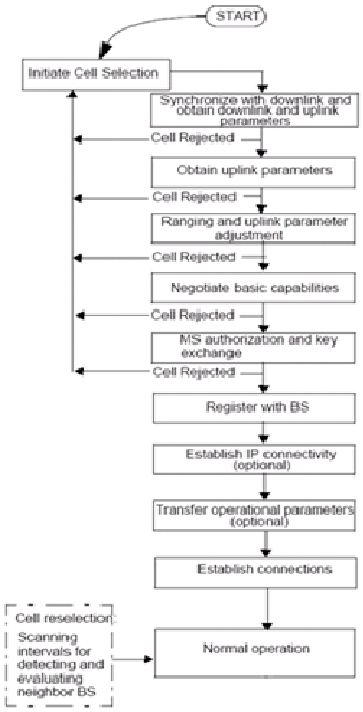

Figure 2: Initialization and registration procedure.

After this setup is completed, a SS can create one or more connections over which its data are transmitted to and from the BS. SSs request transmission opportunities using the UL sub-frame. The BS collects these requests and determines the number of OFDMA symbols (grant size) that each SS will be allowed to transmit in the UL sub-frame. This information is broadcasted in the DL channel by the BS in each DL sub-frame. The UL-MAP frame contains Information Elements (IE) which describes the use of the UL-Frame, including maintenance, contention and reservation access. After receiving the UL-MAP, a SS will transmit data in the predefined reserved OFDMA symbols indicated in the IE. These OFDMA symbols represent transmission opportunities assigned by the BS using a QoS Service class such as UGS (Unsolicited Grant Service) for CBR (Constant Bit Rate) traffic, rtPS (real-time Polling Service) for VBR (Variable Bit Rate), nrtPS (non real-time Polling Service) for non real-time bursty traffic, and BE (Best Effort) for traffic such as Internet, email and all other non real-time traffic. It is important to note that IEEE 802.16 systems have great flexibility regarding the configuration of the UL sub-frame.

3.2 Performance analysis for VoIP traffic

In this section, we present a performance analysis of the IEEE 802.16e MAC protocol when VoIP traffic is being transmitted using a 20 MHz channel. The theoretical model that we have derived for the performance analysis can also be used to study other applications. This study, however, evaluates Constant Bit Rate traffic to stress the network with short VoIP packets when the UGS service class is used. From Figure 1, we can see that the DL sub-frame is comprised of a Preamble, a FCH sub-frame, a DL-MAP sub-frame, a UL-MAP sub-frame and DL bursts. According to the standard [12], all of these sub-frames, with the exception of the DL-MAP and the UL-MAP, are constants. Here the DL bursts are constant since they are used to transport fixed-size VoIP frames. Therefore, we just need to compute the available number of OFDMA symbols at the PHY layer per second ($AvailSym_{DL}$) and divide this value by the number of OFDMA symbols per second required by each SS at the PHY layer ($SSVoIP$). This operation results in the number of SSs supported in the DL direction ($VoIPstreams_{DL}$). Similarly, we follow the same procedure to compute the number of SSs supported in the UL direction ($VoIPstreams_{UL}$). Finally, the maximum number of SSs supported (MaxVoIPstreams) in a 20 MHz channel for the transmission of VoIP traffic will be min($VoIPstreams_{DL}$, $VoIPstreams_{UL}$). In order to validate the theoretical model, we used a simulation model based on the OPNET Modeler Simulation Package V.14.5.

A) Theoretical Model

To model the IEEE 802.16e protocol, we used the parameters given in Table 1. These parameters include the default values given by the standard [10]. The available number of OFDMA symbols per second in the DL direction is given by equation (1). The 1-OFDMA symbol has been taken out of the Preamble.

$$AvailSymb_{DL} = \frac{1}{Frame_d}\left[\begin{matrix}(OFDMAsymb_{DL} - 1) * \\ DataSubCarr_{DL} - MapZoneSize\end{matrix}\right] \quad (1)$$

The *MapZoneSize* provides the number of OFDMA symbols that are consumed by the FCH, DL-MAP and UL-MAP sub-frames as the number of SS increases, which can be computed as:

$$MapZoneSize = \left\lceil \frac{FCH + MapSize_{DL} + MapSize_{DL}}{QMap_{DL}} \right\rceil * QMap_{DL} \quad (2)$$

In (2), we apply the minimum reservation unit called a Quantum MAP (*QMap*) defined in the standard [10], which is given by:

$$QMap_{DL} = QSymb_{DL} * SubCarr_{psubch\,DL} \quad (3)$$

Parameter	Default Value	
Frame Duration ($Frame_d$)	5*ms*	
FCH Symbols (FCH_{symb})	2	
FCH Sub-Channels (FCH_{subch})	1	
Symbols for Ranging HO ($RangSymb_{HO}$)	2	
Sub-Channels for Ranging Handoff ($RangSubCh_{HO}$)	6	
Symbols for Ranging and BW request ($RangQSymb_{BW}$)	1	
Sub-Channels for Ranging and BW request ($RangSubCh_{BW}$)	6	
Repetition Count DL MAP (*RepCount*)	4	
Number of Active Subscriber Stations (N)	[2-800]	
	Sub-*frame*	
	UL	**DL**
Data Sub-Carriers (*DataSubCarr)*	1120	1440
Sub-Channels (*SubCh)*	70	60
Quantum Symbol Size (*QSymb*)	3	2
Quantum Map Size (*QMap*)	48	48
Information Element Size in bits ($IEsize_{bits}$)	32*8	60*8
Sub-Carriers Per Sub-Channel ($SubCarr_{psubch}$)	16	24
OFDMA Symbols (*OFDMAsymb*)	18 or 21	29 or 26

Table 1: MAC and PHY layer parameters for a 20 MHz Channel.

The FCH sub-frame should be also computed using the minimum reservation unit as:

$$FCH = \left\lceil \frac{FCH_{symb} * FCH_{subch} * SubCarr_{psubch\,DL}}{QMap_{DL}} \right\rceil * QMap_{DL} \quad (4)$$

The MAP size for the DL and the UL directions can be computed by equations (5) and (6), respectively. All the parameters used in equations (1) to (6) are defined in Table 1.

$$MapSize_{DL} = \left\lceil \frac{\left(MACHeader_{bytes} + MapHeader_{bytes\,DL}\right) * 8 + N * IEsize_{bits\,DL}}{QMap_{DL}} \right\rceil * QMap_{DL} * \mathrm{Re}\,pCount \quad (5)$$

$$MapSize_{UL} = \left\lceil \frac{\left(MACHeader_{bytes} + MapHeader_{bytes\,UL} + 2 * IErang_{bytes}\right) * 8 + N * IEsize_{bits\,UL}}{QMap_{UL}} \right\rceil * QMap_{UL} \quad (6)$$

Then, the number of VoIP streams supported in the DL direction is given by:

$$VoIPstreams_{DL} = \frac{AvailSymb_{DL}}{SSVoIP} \quad (7)$$

In order to compute the data rate of VoIP streams (*SSVoIP*), we need to obtain the VoIP frame size at the PHY layer ($VoIPFrame_{PHY}$) and then multiply this frame by the number of VoIP frames per second ($1/\lambda$). We consider only two VoIP codecs G.711 and G723.1 for this analysis, which are described as follows:

1) Codec G.711 [11] was considered to stress the IEEE 802.16e network and because this codec is used for quality voice calls. G.711 is the mandatory codec according to the ITU-T H.323 conferencing standard [12], which uses Pulse Code Modulation to produce a data rate of 64 kbps at the application layer. This codec creates and encapsulates a 80-byte VoIP frame every 10 ms.

2) According to the ITU, IETF and the VoIP Forum, G723.1 (or G.723 from now on) [13] is the preferred speech codec for Internet telephone applications. This codec generates a data rate of 5.3 kbps at the application layer, where a 20-byte VoIP frame is generated and encoded every 30 ms.

VoIP frames at the PHY layer should consider modulation and coding overheads, thus the data rate per SS can be obtained as

$$SSVoIP = \frac{VoIPFrame_{PHY}}{\lambda * M * cc} \quad (8)$$

where λ is the inter-arrival time of VoIP frames, M is the number of bits per symbol (2 for QPSK,4 for 16-QAM , 6 for 64-QAM) and *cc* is the convolutional coding rate. Figure 3 shows the encapsulation process for

G.711 and G.723 codecs using two different modulations (QPSK *cc*=1/2 and 64-QAM *cc*=3/4) . According to [14] and [15], header suppression (HS) is possible where fixed fields of the RTP, UDP and IP headers can be disregarded. This results in a reduction from 40-bytes to 14-bytes of header as shown in Figure 3b and 3d. This reduction of RTP+UDP+IP headers increases system performance as indicated in the following sections.

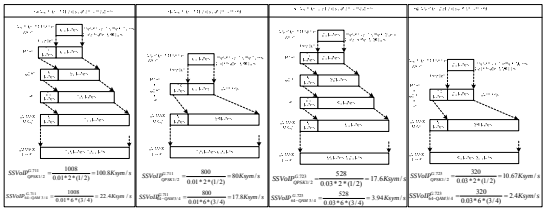

Figure 3: VoIP encapsulation for G.711 and G.723 codecs, with and without header suppression.

The expression to compute the available number of OFDMA symbols in the UL direction is simpler, as indicated in equation (7).

$$AvailSymb_{UL} = \frac{1}{Frame_d}\left[\begin{array}{l}\left(\left\lfloor\frac{OFDMAsymb_{UL}}{QSymb_{UL}}\right\rfloor * QSymb_{UL} * DataSubCarr_{UL}\right) \\ -RangQSymb_{HO} * RangSubCh_{HO} * SubCarr_{psubchUL} \\ -RangQSymb_{BW} * RangSubCh_{BW} * SubCarr_{psubchUL}\end{array}\right] \quad (9)$$

In (7), we assume that the UL sub-frame also includes some ODFMA symbols for the transmission of handoff messages. Thus, the number of VoIP streams supported in the UL direction is given by:

$$VoIPstreams_{UL} = \frac{AvailSymb_{UL}}{SSVoIP} \quad (10)$$

Finally, the maximum number of VoIP streams supported is given by:

$$MaxVoIPstreams = \min(VoIPstreams_{DL}, VoIPstreams_{UL}) \quad (11)$$

B) Simulation Model

In order to validate the theoretical model, we implemented a WiMAX Mobile simulation model based on the OPNET MODELER package v.14.5. A hierarchical design was used which is shown in Figure. 4. At the top level of the IEEE 802-16e network model are the network components, including the Base Station, SSs and servers, as shown in Figure 4a. The next hierarchical level, Figure 4b, defines the functionality of a SS in terms of components such as traffic sources, TCP/UDP, IP, MAC and PHY, interfaces, etc. The operation of each component is defined by a Finite State Machine (an example of which is shown in Figure. 4c). The actions of a component at a particular state are defined in Proto-C (see Figure 4d). This approach allows modifications to be applied to the operation of the IEEE 802.16.e MAC protocol and different optimizations and enhances to be tested. The parameters used for the simulation model were the same as the theoretical model defined in Table 1.

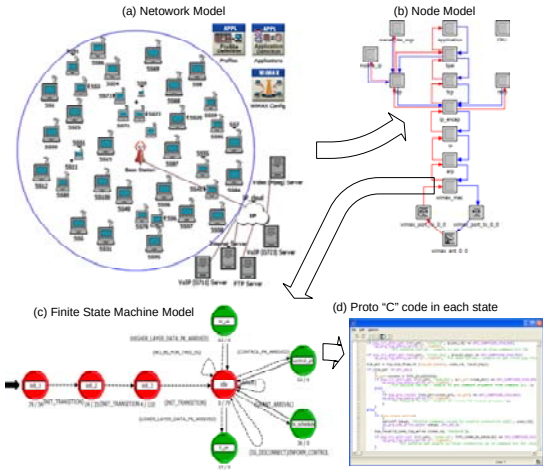

Figure 4: IEEE 802-16e simulation model.

C) Results

The performance analysis of VoIP traffic in a WiMAX Mobile network is of great importance for the 4G Telecommunications community. This study will determine the maximum number of SS that can support a VoIP phone call so that a WiMAX Mobile network, when being implemented in a real-life scenario, is not overloaded. Having an over-dimensioned network would result in a lower system performance.

We modeled a 20 MHz TDD channel for the performance analysis, using the configuration parameters as indicated in Table 1. We evaluated two different codecs (G711,G723) and we employed two modulations for each codec: QPSK with convolutional coding = ½ (QPSK1/2) and 64-QAM with convolutional coding = ¾ (64-QAM3/4). The data rates of VoIP frames at the PHY layer in [ksym/s] with/without header suppression is illustrated in Figure 3 (lower part).

Figures 5 and 7 show the network performance in terms of system throughput and mean access delays, respectively, using the simulation and theoretical model. We considered different frame configurations in order to optimize the system throughput and increased the number of VoIP streams supported. Thus, the codecs in figures 3a and 3d were modeled with DL-OFDMAsym = 29 and UL-OFDMAsymb = 18, and codecs in figure 3b and 3c were modeled with DL-OFDMAsym = 26 and UL-OFDMAsymb = 21.

Figure 5a illustrates the throughput for the UL direction. The same throughput was true for the DL direction, thus Figure 5a also applies for the downlink. The maximum number of quality phone calls in a 20 MHz channel is 38 (this is the result of having 38 outgoing VoIP streams in the UL sub-frame and 38 ingoing VoIP streams in the DL subframe), using codec G.711 with the modulation of QPSK1/2. When HS is considered, this number increases by 26.3%, so *MaxVoIPStreams*=54. By changing the modulation to 64-QAM3/4, we have *MaxVoIPStreams* = 144 without HS and 160 with HS. Here, the increase is 11.1% compared with 26.3% of QPSK1/2. This difference can be attributed to the waste of symbols when QSPK1/2 was used. Figure 6 shows the allocations of VoIP bursts in either direction, where the empty space could not be allocated for the transmission of VoIP traffic, since it is not possible to have fragmented VoIP frames when UGS is used. However, most of this empty space is allocated for the transmission of more VoIP bursts when 64-QAM3/4 is considered, because VoIP bursts are significantly reduced and can fit better in the unscheduled symbols. Moreover, the reduction in throughput when HS, considered in Codec G711-64-QAM3/4, is attributed to the DL-MAP and UL-MAP sub-frames, which increase as the number of SSs increases, thus reducing the throughput from 13.8 Mbps (=144SSs*96Kbps, where DL-MAP+UL sub-frames = 4.031Msym/s) to 12Mbps (160SSs*75.2Kbps, where DL-MAP +UL-MAP sub-frames =5.184Msym/s).

Similarly, Figure 5b shows the UL throughput of G723, which also applies to the DL direction. We observe that the maximum number of phone calls increases considerably to *MaxVoIPStreams* = 226 without HS and 354 with HS, when QPSK ½ is considered. Importantly, the phone calls are performed with a medium quality where MOS (Mean Opinion Score) = 3.6, compared to MOS= 4.4 in G711. By using 64-QAM3/4, the number of phone calls increases to 600-HS and 738+HS. This analysis can be directly applied to fixed nodes where the modulation type can be negotiated with the BS at connection setup. Importantly, for mobiles nodes, QPSK ½ is recommended for bandwidth estimation, along with unscheduled symbols for nrtP or BE services.

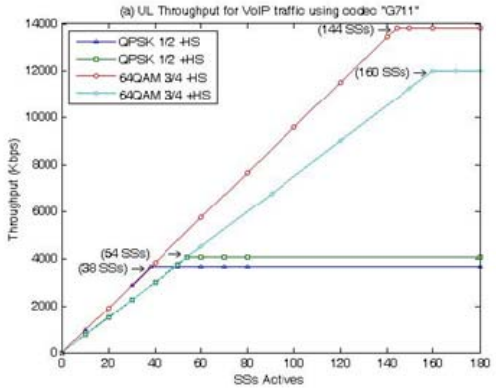

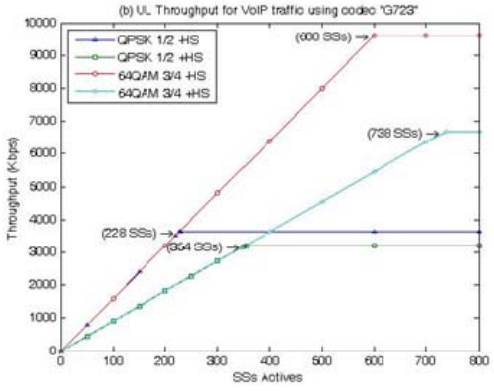

Figure 5: Maximum system throughput of VoIP traffic in a 20 MHz channel.

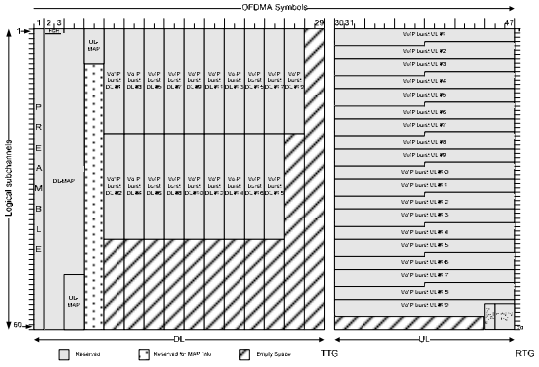

Figure 6: MAP and VoIP burts allocation for codec G711-QPSK1/2.

Finally, Figure 7 shows the mean access delay of VoIP frames in the UL direction. According to **"**PacketCable™ Audio/Video Codecs Specification" **[**16], in order to estimate the one-way delay we need to know: 1) Coding delay (comprised of Encoding and Decoding delays), 2) Access delay (comprised of MAC access delay+ transmission delay + propagation delay), and 3) Look-ahead delay. The coding and look-ahead delays are constant and are 20 ms and 67 ms for codec G711 and G723, respectively. In Figure 7a, for codec G711, we see that the mean access delays are between 9 and 14 ms. Also, coding + look-ahead delays the point to point (PtP) delay which becomes 39-44ms, significantly under the maximum 150ms PtP delay allowed for VoIP calls. For codec G723, as shown in Figure 7b, the mean access delay is between 18 and 26ms. This delay becomes 85.5-93.5 ms when coding + look-ahead delays are considered, which is still below the maximum PtP delay.

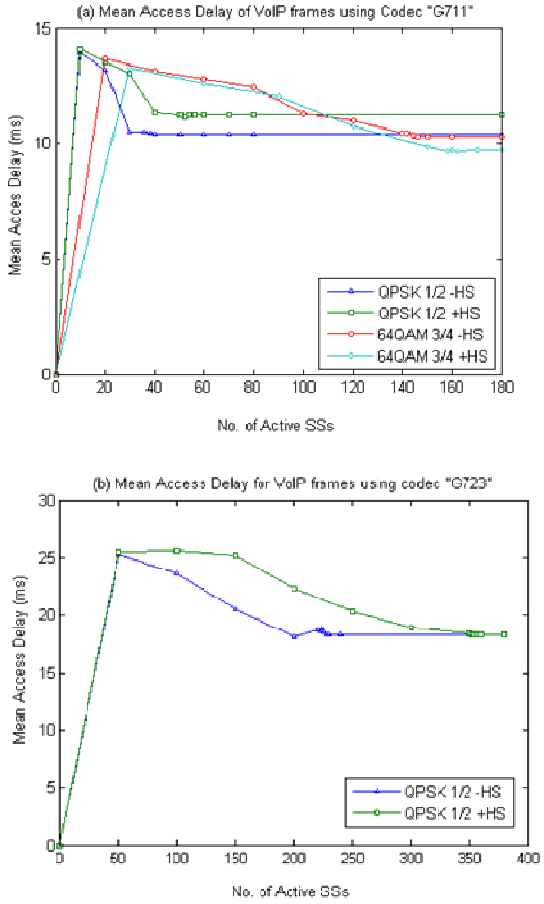

Figure 7: Mean Access Delay of VoIP traffic in a 20 MHz channel.

D) Discussions and Conclusions

The performance analysis presented in this section indicates that VoIP streams under different configurations can be supported by the WiMAX Mobile protocol. There are, however, performance issues that need to be considered. The general trend from the results is that the system will comfortably support a number of active SSs transmitting one UL VoIP stream and one DL VoIP stream, where the maximum system throughput is obtained at the point when all available OFDMA symbols are scheduled.

After that point, even a slight increase in the number of SSs results in system instability. Performance deterioration is not gradual and the packet access delay increases rapidly after the threshold point if there is no control over the traffic accepted. Results shown in Figure 7 were obtained using a call admission control (CAC) scheme at the call setup (using the simulation model) that computes the available number of OFDMA symbols in each direction (DL and UL). A new call is accepted if there are enough available OFDMA symbols to allocate *SSVoIP* [sym/s] in each direction. In general, the use of header suppression considerably increases bandwidth, achieving a much higher figure regarding the maximum number of sustainable streams. In *addition*, by considering compressed RTP (cRTP), the RTP, UDP and IP headers can be reduced to only two bytes where no UDP chechsums are sent or four bytes when UDP checksums are employed. Moreover, system performance highly depends on the repetition count (*RepCount*). In the performance analysis we used the default value *RepCount* =4. However, we can increase the number of VoIP-G723 phone calls to approximately 900 by combining a *RepCount* = 2 with cRTP. Further research will focus on a performance analysis of VoIP with mobile SSs considering codecs G728 and G729 with cRTP (RFC 2508) and with silence suppression to reduce VoIP bandwidth by 60%.

4. Mobile Ad hoc Routing Algorithms

A Mobile Ad Hoc Network (MANET) is formed by a collection of mobile nodes which communicate using the wireless medium. Additionally, a MANET is defined as an autonomous network that has no single point of coordination. These types of networks are characterized by dynamic topologies and limited bandwidth. Usually, mobile nodes also suffer from restricted energy consumption as they require batteries. In a MANET, each mobile node (MN) can transmit information using a direct link or a multi-hop link to propagate packets to a destination node. Consequently, all the mobile nodes in a MANET must efficiently implement the employed routing algorithm.

MANET routing algorithms can be classified into two different categories: non-positional algorithms and positional algorithms. Non-positional algorithms can be further classified as proactive (table-driven), reactive (on-demand), or hybrid. Proactive, or table-driven algorithms, periodically update the network topology information, making routes immediately available when needed. The disadvantage of these algorithms, however, is that they require additional bandwidth to periodically transmit topology traffic, resulting in significant network congestion because each individual node must maintain the necessary routing information and is responsible for propagating topology updates in response to instantaneous changes in network connectivity [17]. Important examples of non-positional protocols include Optimized Link State Routing (OSLR) [18] and Topology Dissemination Based on Reverse Path Forwarding (TBRPF) [19]. These two protocols record the routes for all of the destinations in the ad hoc network, resulting in minimal initial delay (latency) when communicating with arbitrary destinations. Such protocols are also called proactive because they store route information before it is actually needed and are table driven because the information is available in well-maintained tables.

On the other hand, on-demand, or reactive protocols, acquire routing information only as needed. Reactive routing protocols often use less bandwidth for maintaining route tables. The disadvantage of these protocols, however, is that the Route Discovery (RD) latency for many applications can substantially increase. Most applications may suffer delay when they start because a destination route must be acquired before communication can begin. On-demand protocols make use of a route discovery process before the first data packet can be sent, resulting in reduced control traffic overhead at the cost of increased latency in

finding the destination route [20]. Examples of reactive, or on-demand protocols, include Ad-Hoc On-Demand Distance Vector (AODV) routing [21], and Dynamic source Routing (DSR) algorithms [22].

A routing protocol that combines both proactive and reactive approaches is called a hybrid routing protocol. The most popular protocol in this category is the Zone Routing Protocol (ZRP) [23]. In ZRP, the network is divided into overlapping routing zones that can use independent protocols within and between each zone. ZRP is considered a hybrid routing protocol because it combines proactive and reactive approaches to maintain valid routing tables without causing excessive overhead. Communication within a specific zone is realized by the Intrazone Routing Protocol (IARP), which provides effective direct neighbor discovery (proactive routing). On the other hand, communication between different zones is realized by the Inter-zone routing Protocol (IERP), which provides routing capabilities among nodes that must communicate between zones (reactive routing).

Scalability represents the principal disadvantage of purely proactive and reactive routing algorithms in highly mobile environments. A second disadvantage is their very low communication throughput, which sometimes results from a potentially large number of retransmissions [24]. To overcome these limitations, however, several new types of routing algorithms that employ geographic position information have been developed, including: Location-Aided Routing (LAR) [25] Distance Routing Effect Algorithm for Mobility (DREAM) [26], Grid Location Service (GLS) [27], Greedy Perimeter Stateless Routing for Wireless Networks (GPSR) [28], Location Routing Algorithm with Cluster-Based Flooding [29], and Geographic Routing Protocol (GRP).

The following sections present a brief description of some of the more representative routing protocols for MANETs.

4.1 AODV

The Ad hoc On-demand Distance Vector (AODV) [21] is a reactive routing protocol that uses different control messages to enable the communication of the mobile nodes. The topology control messages include: Route Request (RREQ), Route Reply (RREP), Route Error (RERR) and optionally a Hello message. This routing protocol tries to find the shortest route possible using the hop count metric.

When a mobile node wants to communicate with another node, and does not already have a valid route to that node, it initiates a route discovery process to locate it. The route discovery process begins with the source node broadcasting a RREQ message to its neighbors; these neighboring nodes will rebroadcast the RREQ message and the process will continue until a RREQ packet finds a destination node or an intermediate node with an active route to the destination. A reverse path (i.e. toward the sender node) is created during the flooding of the RREQ message. When the RREQ message reaches a destination node, a unicast RREP message is sent back to the source node. Importantly, the RREP message uses the reverse path to reach the source node. As the RREP message travels back to the source node, a forward route is created along the intermediate nodes which propagate the RREP message. Upon receiving the RREP message, the source node can begin sending data to the destination node using the path that has been setup during the route discovery process. Figure 8 illustrates the transmission of control messages during the route discovery process.

AODV also relies on the RERR message to report any problem along an established and active route. A source node must discover a new route upon receiving a RERR message.

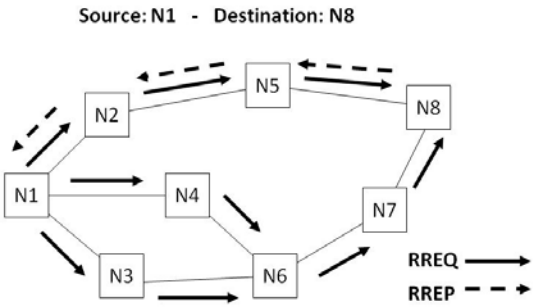

Figure 8: AODV Route Discovery Process

AODV also relies on the RERR message to report any problem along an established and active route. A source node must discover a new route upon receiving a RERR message.

4.2 **DSR**

The Dynamic Source Routing (DSR) protocol [22] is an on-demand protocol designed to reduce the overhead introduced in the network due to the transmission of control massages. This protocol uses a route cache on each node to store routing information within the MANET. The DSR protocol then makes use of its route discovery and route maintenance procedure.

When a mobile node needs to communicate with a destination node, it first checks its route cache for a valid route. If no valid route information is found, the node triggers a route discovery procedure and a *RouteRequest* packet is broadcast. As the *RouteRequest* packets travels though the MANET, the intermediate nodes check their route cache. If no valid route is found, the intermediate node proceeds to add its own address to the *RouteRequest* packet and then rebroadcasts the packet in the network. In this way, each *RouteRequest* packet carries information regarding the path it has traversed. The *RouteRequest* packet carries a sequence number generated by the source node. This information is used to prevent loop formations and to avoid multiple retransmissions of the same *RouteRequest* by the intermediate nodes.

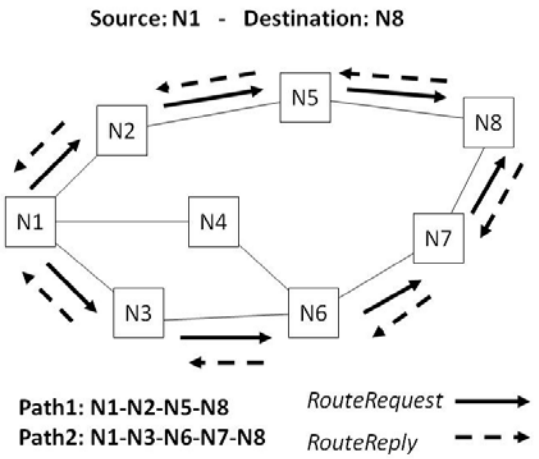

Figure 9: DSR Route Discovery Process

Once the *RouteRequest* message reaches the destination or an intermediate node with a valid route to the destination, a *RouteReply* message is sent back to the source node using the reverse path information carried in the *RouteReply* message. If the *RouteReply* message is generated by the destination node, it proceeds to add the traverse route information from the *RouteRequest* message into the *RouteReply* message. If the *RouteReply* is sent by an intermediate node with a valid route in its route cache, then it replies to the source node by including the entire route information from the source node to the destination. Figure 9 illustrates the propagation of the *RouteRequest* and *RouteReply* messages during the route discovery phase.

The route maintenance procedure is achieved with the aid of the *RouteError* message. A *RouteError* message is sent to the source node whenever a problem is detected at the data link layer, thus signaling the broken link along the route.

4.3 OLS

The Optimized Link State Routing (OLSR) is defined as a proactive routing mechanism for mobile ad hoc networks [18]. It optimizes the pure link state protocol by propagating the topology information via selected nodes,

which are called multi-point relays (MPRs). In the OLSR protocol, the algorithm relies on the propagation of two control messages to propagate topology information: the Hello message and the Topology Control (TC) message

Each node in the MANET will periodically transmit a Hello message to identify itself to any one-hop neighbor node. In addition, the Hello message includes information about the one-hop neighbors of the node transmitting the Hello message. As the MN receives the Hello messages, it can create a one-hop neighbors list, as well as a two-hop neighbors list. By using the OLSR topology lists, a MN can proceed to select a subset of one-hop neighbor nodes which will become multi-point relay nodes (MPR).

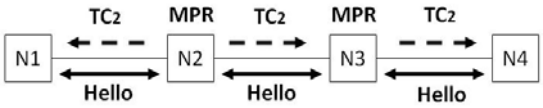

Figure 10: OLSR control messages: Hello and TC

The selection of MPR nodes follows a heuristic algorithm where the main objective is to create a subset of one-hop neighbor nodes that can provide connectivity (i.e. routing) to the complete set of two-hop neighbor nodes. A description of the MPR selection algorithm can be consulted in 0. The OLSR protocol relies on the MPR nodes to periodically transmit TC messages which are used to announce who has selected them as an MPR. Such messages are relayed by other MPRs throughout the entire network, enabling the remote nodes to discover the links between an MPR and its selectors. Based on such information, the routing table is calculated using the shortest-path algorithm. Figure 10 illustrates the control message exchange in OLSR.

4.4 **TORA**

The Temporally Ordered Routing Algorithm (TORA) is a highly adaptive, loop-free, distributed routing algorithm based on the concept of link reversal [25]. TORA is a source-initiated protocol that has been designed for highly dynamic mobile network environments where topology is expected to change frequently over time. To support operation over such dynamic environments, TORA is capable of establishing multiple routes for any desired source-destination pair. To accomplish this, each node needs to maintain routing information about neighboring (1-hop) nodes. The routing protocol relies on three basic functions: route creation, route maintenance and route erasure.

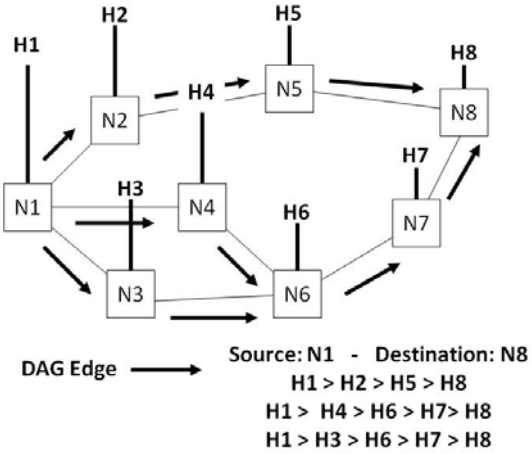

Figure 11: TORA Route Creation Procedure.

As part of the route creation and maintenance procedures, each node uses a "height" metric to construct a directed acyclic graph (DAG) that is rooted at the destination node. As a result, multiple paths between a source and a destination node can be established based on the links that are assigned a direction (i.e., upstream or downstream), based on the relative height of the intermediate routing nodes. The construction of the DAG is similar to the query/reply process of the Lightweight Mobile Routing (LMR) protocol. Figure 11 provides an example of the route creation procedure.

As the mobile nodes change their relative positions, the network topology changes and the DAG links can break. TORA implements a route maintenance mechanism which is

executed upon detection of a broken link. A node which detects a broken link will change it height metric to reflect a new reference level with its neighboring nodes, which results in the propagation of that reference level by neighboring nodes. As a result, the reverse path links to neighboring nodes are maintained. Upon detection of invalid routes, a mobile node may broadcast a clear packet (CLR) to erase invalid routes.

4.5 LAR

The Location Aided Routing (LAR) protocol [25] is a reactive protocol where the mobile nodes have location (or geographic) information. LAR estimates the destination's location to restrict the flood to a small region (called request zone) relative to the whole network region [30].

LAR's basic strategy is to estimate the position of a destination node based on a prior route discovery of that node. Then, based on the estimated position, the source node proceeds to flood limited areas to facilitate subsequent route discovery. As the route discovery message propagates, neighboring nodes evaluate their own distance towards the destination's location in the request. If the intermediate node is closer to the destination than the source node, the message gets forwarded. On the other hand, if the intermediate node is farther away from the destination node than the source, the request gets discarded. This procedure is repeated by other intermediate nodes to create a directed flooding of the route discovery message which is then propagated toward the estimated destination location. It should be noted that LAR only employs geographic forwarding during the route discovery stage and it is not employed during the forwarding of data packets [30]. Figure 12 illustrates the route discovery procedure employed by LAR.

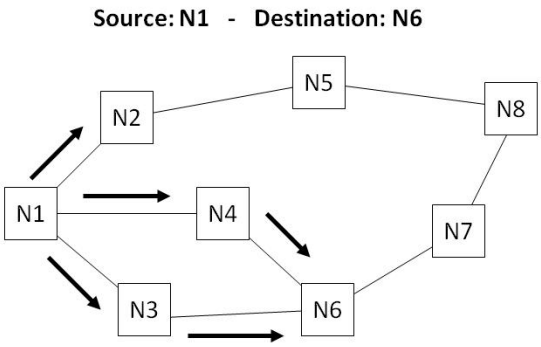

Figure 12: Route discovery procedure in LAR.

5. Microscopic Traffic Simulation Model

Vehicular Traffic models may be categorized according to the level-of-detail into four classifications: sub-microscopic, microscopic, mesoscopic, and macroscopic [31]. The sub-microscopic models describe the characteristics of individual vehicles in the traffic stream and the operation of specific parts (sub-units) of the vehicle. Microscopic models simulate each driver behavior and the interaction among drivers; the implemented algorithms are very detailed and allow tracking explicitly the space-time trajectory of each vehicle [32]. Mesoscopic models represent the transportation systems analyzing group of drivers having homogeneous behavior. Finally, macroscopic models describe traffic at a high level of aggregation as a flow without distinguishing its basic parts [33]. Because, we are interested in the space-time trajectory of each vehicle governed by the vehicle in front, this chapter will focus on microscopic traffic models.

A large number of microscopic traffic simulation models have been developed. Basically, these models describe the time-space behavior of the vehicles in the traffic system.

The microscopic traffic simulation model used in this work for evaluating the performance of several mobile routing algorithms is based in a constant flow.

6. Simulated scenario

The scenario used in this study is a circular road model representing a highway topology. This kind of scenario allows messages to be transmitted only between vehicles that move along the highway. In this way, all of the vehicles remain in the scenario, while preserving a constant vehicular density and distribution.

The circular scenario represents a typical 4-lane highway in Mexico with two lanes in one direction and two others in the opposing direction. The vehicles in the exterior lanes flow clockwise and the interior two lanes flow counterclockwise. Each lane has a ten-meter width and the exterior radius of the outside lane is 3 kilometers.

The scenario has no entrances or exits. The simulation has a total of 100 vehicles, 25 per lane. The exactly location of each node can be calculated with the equation (12) that represents the parametric equation of the circumference with the parameter X= ρ·cos Ω, where ρ is the radius of the correspondent lane and Ω is an angle that grows from 0° to 360° in increments of 14.4° and (x',y') is the center of all lanes.

$$(x - x')^2 + (y - y')^2 = \rho^2 \qquad (12)$$

The separation between vehicles and those immediately following in the same lane have a uniform distribution of less than a kilometer. More precisely, the distance between each vehicle is calculated with (13), where ρ is the radius of each lane. To preserve the distance between vehicles, all of them move at a constant speed of 42 m/s, having an approximate relative speed of 300 km/h between vehicles moving in opposite directions. Figure 13 shows details of the scenario designed for this study.

$$s = \frac{2 \cdot \pi \cdot \rho}{25} \qquad (13)$$

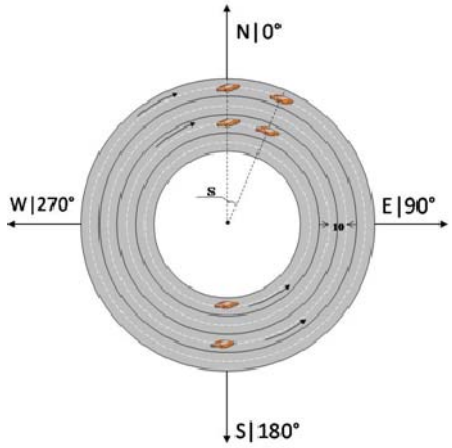

Figure 13: Simulated scenario

The OPNET MODELER package v.14.5 was used to simulate a constant microscopic traffic model which requires two main parameters: angle and speed. The angle between the actual and final positions correspond to actual compass headings from 0 to 360°, where 0° represents north, 90° is east, 180° is south and 270° is west. Besides the angle, vehicle speed must also be kept constant. To allow the vehicles to flow in a circular trajectory, angle α between the actual position and the next position in the perimeter of the circumference must be calculated as accurately as possible. Importantly, if the node's position is other that 270°, an offset β must be added to the angle. Figure 14 shows a graphical representation of the two angles that must be found.

Calculating the β offset is an easy task using the dot product if one knows the two vectors involved. These can be calculated with the actual position of the node, the initial reference (0°) and the center of the circumference. If the initial reference and the center of the circumference are known, OPNET API can easily calculate the actual position. Angle α can also be easily calculated with simple geometry and (3).

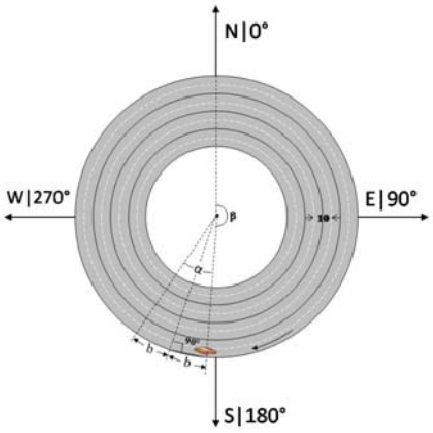

Figure 14: Graphical representation of two angles.

$$\alpha = \frac{2 \cdot b \cdot 100}{\pi \cdot \rho} \quad (3)$$

The angle units are obtained in degrees where ρ is the radius of the vehicle's lane and b is the length of the arc that we want cover.

7. Simulation metrics

Packet delivery ratio: is the ratio of data packets delivered to the number of data packets sent by the source. Data packets, however, may be dropped if the link is broken when the data packet is ready to be transmitted.

MANET delay: is all of the possible delays caused by buffering during route discovery, queuing at the interface queue, re-transmission delays at the MAC layer, and propagation and transfer times.

Routing overhead: is the total number of routing packets transmitted during the simulation.

Routing load: is the number of routing packets transmitted per data packet transmitted. The later includes only the data packets finally delivered at the destination and not the ones that are dropped. The transmission at each hop is counted once for both routing and data packets. This provides an idea of network bandwidth consumed by routing packets with respect to "useful" data packets.

Overhead: is the total number of routing packets that are generated divided by the total number of data packets transmitted, plus the total number of routing packets.

WiMAX delay: is measured at the MAC layer. This is different for the MANET delay, which is measured at the network layer. Both delays are peer to peer.

WiMAX load: is defined as the total load (in bits/sec) submitted to the WiMAX layer by all higher layers in all network WiMAX nodes.

WiMAX throughput: is the total data traffic (in packets/sec) forwarded from WiMAX layers to higher layers in all network WiMAX nodes.

8. Simulation results

Figure 15 presents the packet delivery ratio for AODV and OLSR at a speed of 150 km/h in each direction (relative speed of 300 km/h). During the simulation, data packets begin at 100 seconds and they are sent at 1-second intervals (constant bit rate), employing a 1024-bit packet size. The source vehicle and the destination vehicle are located opposite each other in the scenario (Figure 13) so that data packets must travel several hops. AODV and OLSR present a very low packet delivery ratio because these types of routing algorithms are not very efficient in high mobility applications.

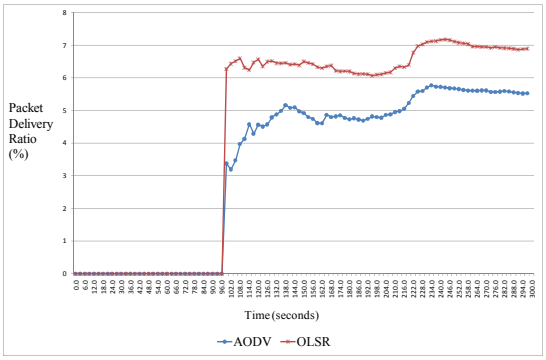

Figure 15: Delivery ratio for AODV and OLSR.

MANET delay is presented in Figure 16. AODV shows higher MANET delay because AODV is a reactive routing algorithm. Reactive routing algorithms require a discovery process before they can transmit their data packets. On the other hand, OLSR is classified as proactive routing algorithm. Proactive routing algorithms maintain the routing information of all possible destinations in a table, which significantly improves MANET delay.

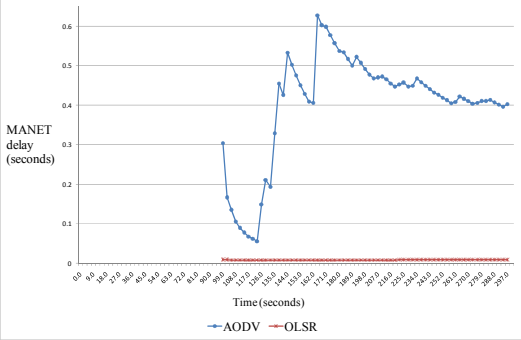

Figure 16: MANET delay for AODV and OLSR.

Figure 17 presents the routing overhead. AODV has a higher routing overhead, which increased during the simulation. On the other hand, the routing overhead on OLSR is more stable. It is important to add that stability is a basic requirement of highly mobile applications.

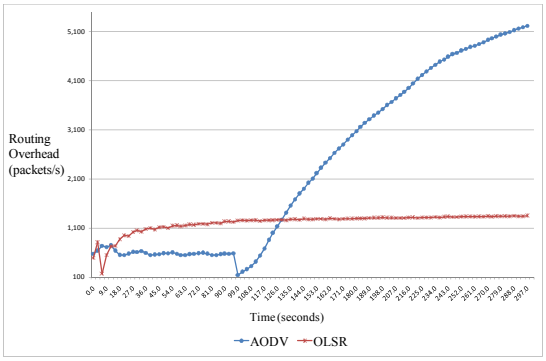

Figure 17: Routing overhead for AODV and OLSR.

Figure 18 shows Overhead, which is the algorithm's bandwidth consumption. AODV presents more overhead because reactive algorithms must initiate the discovery process when links are broken. This frequently discovery process can flood the network with routing packets. OLSR, on the other hand, presents low overhead because it is a proactive algorithm that keeps the routing information of all possible destinations in a routing table. If there is a broken link, OLSR does not need to flood the network, which serves to minimize overhead.

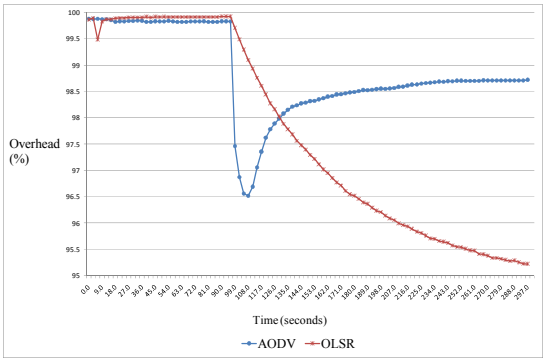

Figure 18: Overhead for AODV and OLSR.

WiMAX delay is presented in Figure 19. AODV is lighter because of its reactive nature; its routing process only begins when the source vehicle needs to send data packets to the destination vehicle. On the other hand, proactive algorithms are constantly sending routing information, even though they are not sending data packets.

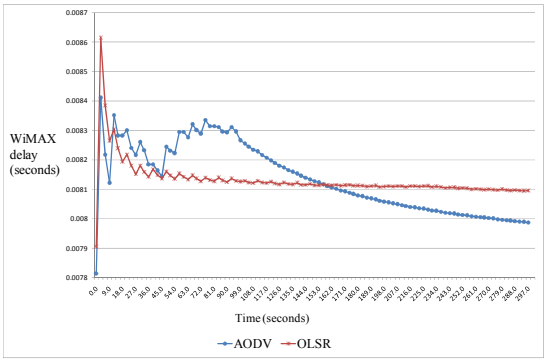

Figure 19: WIMAX delay for AODV and OLSR.

Figure 20 shows the WiMAX load. As described previously, proactive algorithms need to constantly send routing information even though they are not transmitting data packets, which cause OLSR to have a higher WiMAX load.

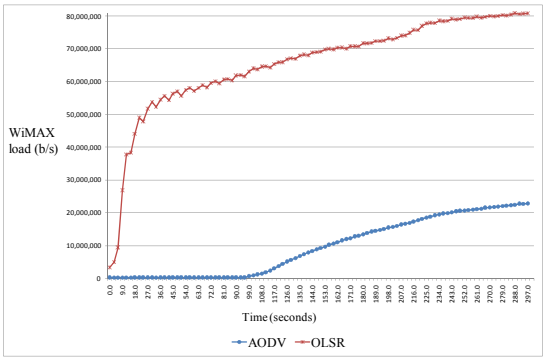

Figure 20: WiMAX load for AODV and OLSR.

WiMAX throughput is presented in Figure 21. AODV shows better throughput because of its reactive nature. AODV only starts its routing mechanism when it needs to send data packets. On the other hand, OLSR constantly uses network bandwidth, which results in lower throughput.

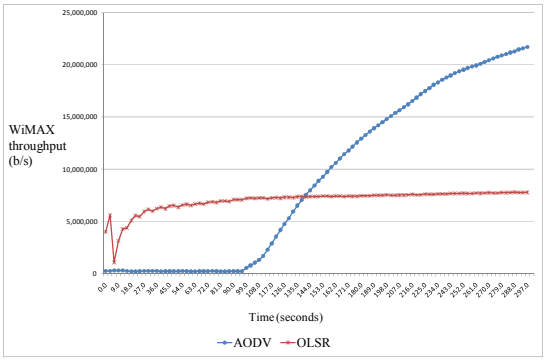

Figure 21: WiMAX throughput for AODV and OLSR.

CONCLUSIONS

This chapter presented the performance evaluation of two prominent mobile ad hoc routing algorithms, AODV and OLSR, over a WiMAX mesh network. The WiMAX and the constant microscopic traffic model were simulated in OPNET. OLSR performs better in terms of packet delivery ratio, MANET delay, routing overhead and overhead. On the other hand, AODV performs better in terms of WiMAX delay, load and throughput. In summary, OLSR is more efficient in terms of network routing, however, its proactive nature affects several WiMAX important metrics at the MAC layer. Our future work will propose a routing algorithm that is more efficient at network and MAC layers.

ACKNOWLEDGEMENTS

This work was supported by DGAPA, National Autonomous University of Mexico (UNAM) under Grant PAPIIT IN104907 and PAPIME PE 103807.

REFERENCES

[1] C. H. Rokitansky, C. Wietfeld. Comparison of Adaptive Medium Access Control Schemes for Beacon-Vehicle Communications. IEEE-IEE Vehicle Navigation & Information Systems Conference, pp. 295-299, 1993.

[2] G. Brasche, C. H. Rokitansky, C. Wietfeld. Communication Architecture and Performance Analysis of Protocols for RTT Infrastructure Networks and Vehicle-Roadside Communications. IEEE 44th Vehicular Technology Conference, pp. 384-390, 1994.

[3] H. FüBler, M. Mauve, H. Hartenstein, M. Käsemann, D. Vollmer. Location-Based Routing for Vehicular Ad-hoc Networks. ACM SIGMOBILE Mobile Computing and Communication Review, vol. 7, pp. 47-49, 2003.

[4] C. Lochert, H. FüBler, H. Hartenstein, D. Hermann, J. Tian, M. Mauve. A Routing Strategy for Vehicular Ad-hoc Networks in City Environments. IEEE Intelligent Vehicles Simposium, pp. 156-161, 2003.

[5] B. Bing. "High-Speed Wireless ATM and LANs", Artech House Mobile Communications Library, Norwood, 2000.

[6] IEEE 802.16-2001, "IEEE Standard for Local and Metropolitan Area Networks - Part 16: Air Interface for Fixed Broadband Wireless Access Systems", April 2002.

[7] IEEE 802.16-2004, "IEEE Standard for Local and Metropolitan Area Networks - Part 16: Air Interface for Fixed Broadband Wireless Access Systems", October 2004.

[8] Dave Bayer, "Wireless Mesh Networks For Residential Broadband", National Wireless Engineering Conference San Diego, 4 November, 2002.

[9] Dave Beyer, Nico van Waes, Carl Eklund, "Tutorial: 802.16 MAC Layer Mesh Extension Overview", March 2002.

[10] IEEE 802.16e, "IEEE Standard for Local and Metropolitan Area Networks - Part 16: Air Interface for Fixed BWA Systems", Amendment for PHY and MAC for Combined Fixed and Mobile Operation in Licensed Bands, December 2005.

[11] ITU-T Rec. G.711, "Pulse Code Modulation (PCM) of voice frequencies", ITU-T, Nov. 1988.

[12] ITU-T Rec. H.323, "Packet-based Multimedia Communications Systems", ITU-T, Geneva, Switzerland, Nov. 2000.

[13] ITU-T Rec. G.723.1, "Speech coders: Dual rate speech coder for multimedia communications transmitting at 5.3 and 6.3 Kbit/s", ITU-T, 1996.

[14] Rangel Licea V. Performance Evaluation and Optimisation of the DVB/DAVIC Cable Modem Protocol (Phd. thesis). June 2002.

[15] ETSI ES 200 800 v.1.3.1. Digital Video Broadcasting: Interaction Channel for Cable TV Distribution Systems (CATV). October 2001.

[16] PacketCable, "PacketCable™ Audio/Video Codecs Specification", CableLabs, PacketCable Project, Dec. 2001.

[17] Charles E. Perkins. Ad hoc networking. Addison Wesley. 2000.

[18] T. Clausen, P. Jacquet. "Optimized Link State Routing Protocol (OLSR)", Oct. 2003. [Online] Available: http://www.ietf.org/rfc/rfc3626.txt. [Accessed Sept. 4, 2009].

[19] Richard G. Ogier, Mark G. Lewis, Fred L. Templin. "Topology Dissemination based on Reverse-Path Forwarding (TBRPF)", February 2004. [Online] Available http://www.ietf.org/rfc/rfc3684.txt [Accessed Sept. 10, 2009].

[20] Xukai Zou, Byrav Ramamurthy and Spyros Magliveras. Routing Techniques in Wireless Ad Hoc Networks –Classification and Comparison. Proceedings of the Sixth World Multiconference on Systemics, Cybernetics and Informatics, SCI, pp. 1-6, July 2002.

[21] C.E. Perkins, E.M. Belding-Royer, and S.R. Das, "Ad Hoc On-Demand Distance Vector (AODV) Routing", July 2003. [Online] Available: http://www.ietf.org/rfc/rfc3561.txt [Accessed Sept. 4, 2009].

[22] David B. Johnson, David A. Maltz, Yih-Chun Hu. "The Dynamic Source Routing Protocol for Mobile Ad Hoc Networks (DSR)", February 2007. [Online] http://www.ietf.org/rfc/rfc4728.txt [Accessed Sept. 4, 2009].

[23] Jan Schaumann. "Analysis of the Zone Routing Protocol", December 2002. [Online] http://www.netmeister.org/misc/zrp/zrp.pdf [Accessed Sept. 4, 2009].

[24] Martin Mauve, Jörg Widmer and Hannes Hartenstein, "A Survey on Position-Based Routing in Mobile Ad-Hoc Networks", *IEEE Network Magazine*, 15(6), pp.30-39, November 2001.

[25] Y. Ko, N. H. Vaidya, "Location-Aided Routing (LAR) in Mobile Ad Hoc Networks", in Proceedings of IEEE/ACM Mobicom, pp. 66-75, 1998.

[26] Stefano Basagni, Imrich Chalamtac, Violet R. Syrotiuk. A Distance Routing Effect Algorithm for Mobility (DREAM). MOBICOM 98. Pp. 76-84, 1998.

[27] Jinyang Li, John Jannotti, Douglas S. J. De Couto, David R. Karger, Robert Morris. A Scalable Location Service for Geographic Ad Hoc Routing. ACM Mobicom 2000, pp. 120-130, 2000.

[28] Brad Karp, H. T. Kung. GPSR: Greedy Perimeter Stateless Routing for Wireless Networks. Proceedings of the 6th Annual ACM/IEEE International Conference on Mobile Computing and Networking (MobiCom 2000), pp. 243-254, 2000.

[29] Santos, R. A., Edwards, A., Edwards, R. M. and Seed, N. L. (2005) "Performance evaluation of routing protocols in vehicular ad-hoc networks". International Journal of Ad Hoc and Ubiquitous Computing. Vol.1, Nos. 1/2, pp. 80-91.

[30] Mahesh K. Marina, Samir R. Das, "Routing in Mobile Ad Hoc Networks", Ad Hoc Networks Technologies and Principles, Eds. Prasant Mohapatra, Srikanth Kirishnamurthy, Springer, pp. 63-90, 2004.

[31] S. P. Hoogendoorn, H. L. Bovy. State of the art of vehicular traffic flow modelling. Special issue on road traffic modelling and control of the journal of systems and control engineering, vol. 215, pp. 283-303, 2001.

[32] D. C. Festa, G. Longo, G. Mazzulla, G. Musolino, Experimental analysis of different simulation models for motorway traffic flow. Proceeding of the IEEE Intelligent Transportation Systems Conference, pp. 675-680, 2001.

[33] B. Cvetkovski, L. Gavrilovska. A simulation of a mobile highway traffic. Proceedings of the IEEE VTC conference, pp. 1429-1433, 1998.